

The relevance of neck linker docking in the motility of kinesin

András Czövek, Gergely J. Szöllősi, Imre Derényi

Department of Biological Physics, Eötvös University

Pázmány P. stny. 1A, H-1117 Budapest, Hungary

April 21, 2008

Abstract

Conventional kinesin is a motor protein, which is able to walk along a microtubule processively. The exact mechanism of the stepping motion and force generation of kinesin is still far from clear. In this paper we argue that neck linker docking is a crucial element of this mechanism, without which the experimentally observed dwell times of the steps could not be explained under a wide range of loading forces. We also show that the experimental data impose very strict constraints on the lengths of both the neck linker and its docking section, which are compatible with the known structure of kinesin.

1 Introduction

Kinesin motor proteins execute a variety of intracellular transport functions by transporting cellular cargo along microtubules (MTs) while hydrolyzing adenosine triphosphate (ATP) [6, 4, 7, 24]. These molecular walking machines move in 8-nm steps toward the plus end of microtubules, turning over one ATP molecule per step under a range of loads [17, 23, 26]. Conventional kinesin (kinesin-1) is a homodimer, the monomers of which consist of a head domain (containing a conserved catalytic core), a stalk (through which the monomers form a dimer), and an approximately 13 amino acid long neck linker (connecting the head to the stalk). The neck linker is evolutionarily highly conserved among plus-end directed motors [24] and appears to be crucial for motility [3].

In a kinesin dimer the two stalks form a coiled coil, to which a cargo is attached or, during experiments, a pulling force is applied. The catalytic core of each head

is responsible for binding and hydrolyzing ATP [13, 14, 19]. ATP binding to a MT bound head has been shown to result in a section of the neck linker binding to the head [18, 3, 19, 22], with a consequence of positioning the remaining unbound section (and also the diffusing other head) closer to the forward binding site [17, 15]. Experimental studies [18] of this conformational change (referred to as ‘neck linker docking’) strongly support a scenario wherein an unstructured, random-coil-like neck linker folds onto the core as a result of nucleotide binding – paying a large entropic cost compensated by a large enthalpic gain (both in the order of 50 kJ/mol or $20 k_B T$, where $k_B \approx 1.38 \times 10^{-23}$ J/K is the Boltzmann constant and T denotes the absolute temperature, which we set now to be 293 K).

Neck linker docking is also confirmed by X-ray structures [12, 21], molecular dynamics simulations [8, 11], and fluorescence experiments [16], however, it is still debated whether docking is crucial to the processivity and force generation of kinesin, or just a byproduct of some other mechanism [10]. To address this question we focus on a single state of the dimer, in which one of the heads is bound to the MT and contains an ATP, while the other head (often called the ‘tethered head’) is unbound and contains an ADP (see left cartoon in Fig. 1). To complete a forward step, the tethered head must find and then bind to the forward binding site on the MT (which is about $L = 8$ nm ahead of the bound head).

In a recent optical tweezers experiment Carter and Cross [2] demonstrated that kinesin can take not only forward but also backward steps. The ratio of the number of backward and forward steps increases as the loading force is increased and reaches unity at the stall force of about -7 pN (a negative force means pulling toward the minus end of the MT). At saturating ATP concentration and at zero loading force the steps almost exclusively occur in the forward direction and their duration (which is also called the dwell time) is around 0.01 s. Near the stall force, however, the steps are much slower with a dwell time of about 0.3 s. We note here that in any situation when two alternative processes compete with each other (such as the forward and backward steps of kinesin) the duration of the successful process will be determined by that of the faster one (meaning that the completion of the slower one will take a similar amount of time, but will occur less frequently). So at small loads the forward steps, whereas at loads exceeding the stall force the backward steps will determine the dwell times of the steps in both directions.

The benefit of neck linker docking appears to be clear: in the one head bound state (described above) this conformational change positions the tethered head closer to the forward binding site on the MT (as demonstrated in Fig. 1). However, to underpin the necessity of neck linker docking in a quantitative manner, we examine under what conditions can the tethered head find the binding site within the aforementioned 0.3 s time limit when the -7 pN stall force is applied.

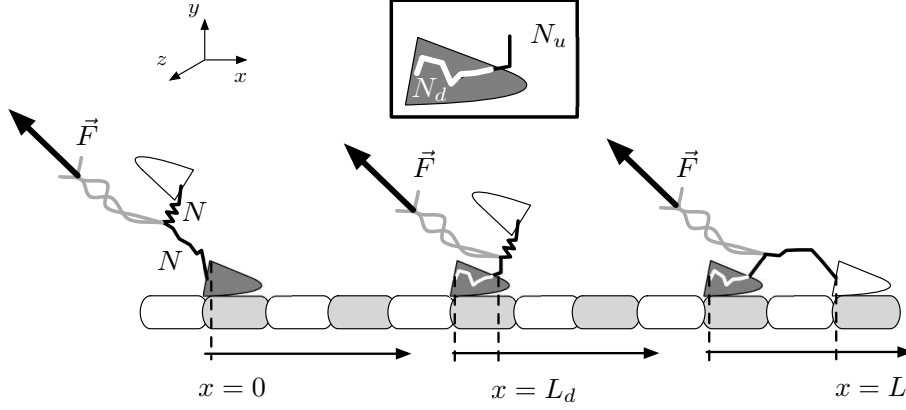


Figure 1: One head bound kinesin before (left) and after (middle) neck linker docking, followed by the binding of the tethers head to the microtubule (right). Inset shows the number of docked neck linker segments (N_d) in white and that of the remaining (N_u) segments of the same neck linker in black.

2 The Model

We suppose that the undocked sections of the neck linkers behave as random coils, which we simply model as freely jointed chains (FJC). Thus, before binding to the MT the tethered head experiences a random walk in the potential of the entropic springs formed by the two connected neck linkers of kinesin. We regard the spatial distribution of the tethered head simply as that of the end of the two joined neck linkers. Each neck linker consists of N_{aa} amino acids ($N_{aa} \approx 13$ for a conventional kinesin). We use $l_{aa} = 0.38$ nm for one amino acid length and $l_p = 0.44$ nm for the persistence length of a polypeptide chain [20]. The Kuhn length is then $l_K = 2l_p = 0.88$ nm, and the number of freely jointed segments in a neck linker is $N = N_{aa}l_{aa}/l_K$, where $N_{aa}l_{aa}$ is the contour length of the polypeptide chain [5]. As one can see this description is quite coarse with respect to the number of amino acids of the neck linker: increasing the number of the segments N by 1 is equivalent to increasing the number of the amino acids N_{aa} by $l_K/l_{aa} \approx 2.3$.

For technical reasons we divide the neck linker of the bound head into two sections. The first one consists of those N_d segments that can dock to the head domain, while the second one contains the remaining $N_u = N - N_d$ segments of the neck linker. The external pulling force \vec{F} acts at the end point of this neck linker, where it joins to the neck linker of the tethered head (as illustrated in Fig. 1). For simplicity we neglect the width and flexibility of the coiled coil stalk between the two neck linkers. This omission could, however, be largely compensated by a slight increase in the length of the neck linkers.

Let x , y , and z be Cartesian coordinates so that the x axis is parallel to the MT, and the x and y axes span the plane of the external force \vec{F} . This way \vec{F} has no z component. The angle of the force (*i.e.*, that of the coiled coil stalk) to the MT depends on the details of the experimental setup, in particular, on the length of the stalk and the size of the bead in the optical trap. Throughout the paper we use a reasonable value of 45° for this angle and, thus, assume that $F_y = |F_x|$. In the experiments, usually the x component of \vec{F} are reported, so by specifying that the stall force is -7 pN we mean $\vec{F} = (-7, 7, 0)$ pN.

Let $\rho_N^0(\vec{R})$ denote the probability density of the end-to-end vector \vec{R} of a free ($\vec{F} = 0$) neck linker with N segments. Such a distribution applies to the neck linker of the tethered head. As $\rho_N^0(\vec{R})$ does not depend on the external force it has a spherical symmetry. The formula for this distribution is derived in the Appendix.

Let $\rho_N(\vec{R}, \vec{F})$ denote the probability density of the end-to-end vector \vec{R} (pointing from the head end of the neck linker towards the pulled end) of the MT-bound head's neck linker with N segments at an applied external force \vec{F} . Note that the applied force breaks the spherical symmetry of the distribution. $\rho_N(\vec{R}, \vec{F})$ can be expressed with the help of $\rho_N^0(\vec{R})$ as

$$\rho_N(\vec{R}, \vec{F}) = \frac{\rho_N^0(\vec{R}) e^{\frac{\vec{F} \cdot \vec{R}}{k_B T}}}{Z_N(\vec{F})} \quad (1)$$

where

$$Z_N(\vec{F}) = \int \rho_N^0(\vec{R}) e^{\frac{\vec{F} \cdot \vec{R}}{k_B T}} d\vec{R} \quad (2)$$

is the partition function.

The compound probability density $\rho_{N_1, N_2}(\vec{R}, \vec{F})$ for the end-to-end vector \vec{R} of two joint neck linkers (with N_1 and N_2 segments, respectively) that are pulled by an external force \vec{F} at the joint (and held fixed at the other end point of the first neck linker) can then be expressed as:

$$\rho_{N_1, N_2}(\vec{R}, \vec{F}) = \int \rho_{N_1}(\vec{R}', \vec{F}) \rho_{N_2}^0(\vec{R} - \vec{R}') d\vec{R}'. \quad (3)$$

By placing the origin of the coordinate system to the starting point of the neck linker of the bound head, the probability density $\rho_{N, N}(\vec{R}, \vec{F})$ can be considered as the concentration of the tethered head at position \vec{R} , given that the neck linker of the bound head is undocked, and if all steric constraints are neglected.

To take the volume exclusion between the tethered head and both the MT (approximated as $R_y < 0$) and the bound head (approximated as $|\vec{R}| < 2$ nm) into account, we introduce a constraining function

$$\Theta(\vec{R}) = \begin{cases} 0 & \text{if } R_y < 0 \text{ or } |\vec{R}| < 2 \text{ nm,} \\ 1 & \text{otherwise.} \end{cases} \quad (4)$$

Multiplying $\rho_{N,N}(\vec{R}, \vec{F})$ by $\Theta(\vec{R})$, and then renormalizing it to unity results in the sterically constrained concentration of the tethered head:

$$c(\vec{R}, \vec{F}) = \frac{\rho_{N,N}(\vec{R}, \vec{F})\Theta(\vec{R})}{\int \rho_{N,N}(\vec{R}, \vec{F})\Theta(\vec{R})d\vec{R}}. \quad (5)$$

Note, however, that the volume exclusion is not imposed on the entire chain, only on its end point. Nevertheless, this steric constraint has very little effect on our main conclusions.

Similarly, denoting the end-to-end vector of the N_d segments of the docked section of the neck linker by $\vec{L}_d = (L_d, 0, 0)$, *i.e.*, assuming that docking occurs in the x direction with a projected distance of L_d , the probability density $\rho_{N_u,N}(\vec{R} - \vec{L}_d, \vec{F})$ can be considered as the concentration of the tethered head at position \vec{R} when that the neck linker of the bound head is docked (and all steric constraints are neglected). After its multiplication by $\Theta(\vec{R})$ and renormalization to unity, results in the sterically constrained concentration

$$c^*(\vec{R}, \vec{F}) = \frac{\rho_{N_u,N}(\vec{R} - \vec{L}_d, \vec{F})\Theta(\vec{R})}{\int \rho_{N_u,N}(\vec{R} - \vec{L}_d, \vec{F})\Theta(\vec{R})d\vec{R}}. \quad (6)$$

Multiplying these concentrations at the positions $\vec{R} = \vec{L} = (L, 0, 0)$ and $\vec{R} = -\vec{L} = (-L, 0, 0)$ by the binding rate constant k_b of the kinesin head, we get the rate at which the tethered head binds to the MT at the forward and backward binding sites, respectively.

The only remaining quantity to determine is the probability of the neck linker being docked or undocked (disregarding the possibility of any long lived partially docked conformation). These probabilities must be a function of the force since the neck linker docks easier if it is pulled forward. Let $P^*(\vec{F})$ denote the probability that the neck linker is docked and $P(\vec{F}) = 1 - P^*(\vec{F})$ that it is not. Then the free energy difference $\Delta G(\vec{F})$ between the docked and undocked state can be defined through

$$\frac{P^*(\vec{F})}{P(\vec{F})} = e^{\frac{-\Delta G(\vec{F})}{k_B T}}. \quad (7)$$

From the measurements of Rice et al. [18] we know that if an ATP is bound to the head, then neck linker docking is an energetically favorable process with a free energy difference of $\Delta G^0 \approx -2k_B T$. Thus, the ratio of the probabilities that the bound head is in the docked and the undocked conformation can be written as

$$\frac{P^*(\vec{F})}{P(\vec{F})} = \frac{e^{\frac{-\Delta G^0}{k_B T}} \int \int \rho_{N_u}^0(\vec{R}' - \vec{L}_d) e^{\frac{\vec{F} \cdot \vec{R}'}{k_B T}} \rho_N^0(\vec{R} - \vec{R}') \Theta(\vec{R}) d\vec{R}' d\vec{R}}{\int \int \rho_N^0(\vec{R}') e^{\frac{\vec{F} \cdot \vec{R}'}{k_B T}} \rho_N^0(\vec{R} - \vec{R}') \Theta(\vec{R}) d\vec{R}' d\vec{R}}. \quad (8)$$

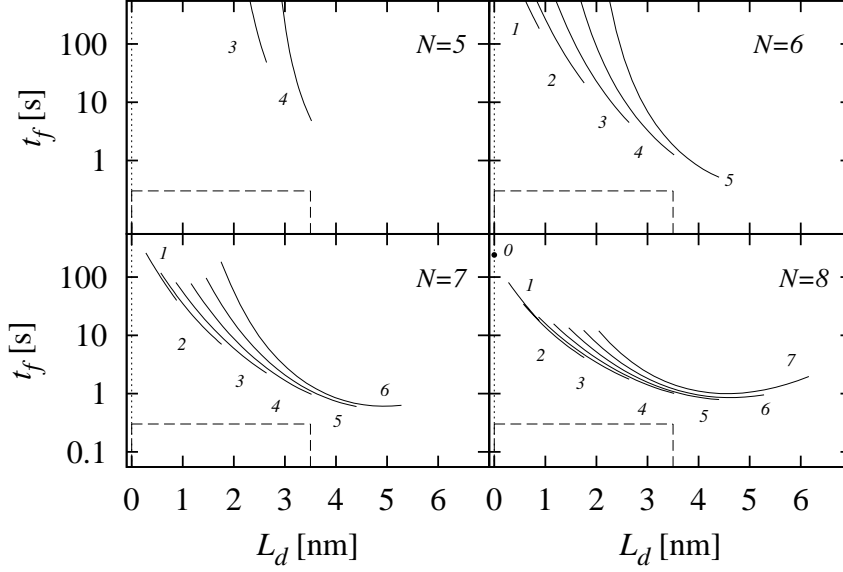


Figure 2: The characteristic time t_f needed to find the forward binding site as a function of the horizontal projection L_d of the docked neck linker at the -7 pN stall force. The four boxes correspond to neck linkers of different lengths with different numbers N of Kuhn segments. The various lines in the boxes correspond to different numbers N_d of docked segments. The rectangular area in the bottom left corner of each box indicates the expected range $t_f < 0.3$ s and $L_d < 3.5$ nm, compatible with the experiments.

The characteristic time for binding forward at force \vec{F} is then:

$$t_f(\vec{F}) = \frac{1}{k_b[P^*(\vec{F})c^*(\vec{L}, \vec{F}) + P(\vec{F})c(\vec{L}, \vec{F})]}. \quad (9)$$

We have no reason to assume a different rate constant k_b for backward and forward binding, therefore, the ratio of the probabilities of forward and backward stepping is:

$$r(\vec{F}) = \frac{P^*(\vec{F})c^*(\vec{L}, \vec{F}) + P(\vec{F})c(\vec{L}, \vec{F})}{P^*(\vec{F})c^*(-\vec{L}, \vec{F}) + P(\vec{F})c(-\vec{L}, \vec{F})}. \quad (10)$$

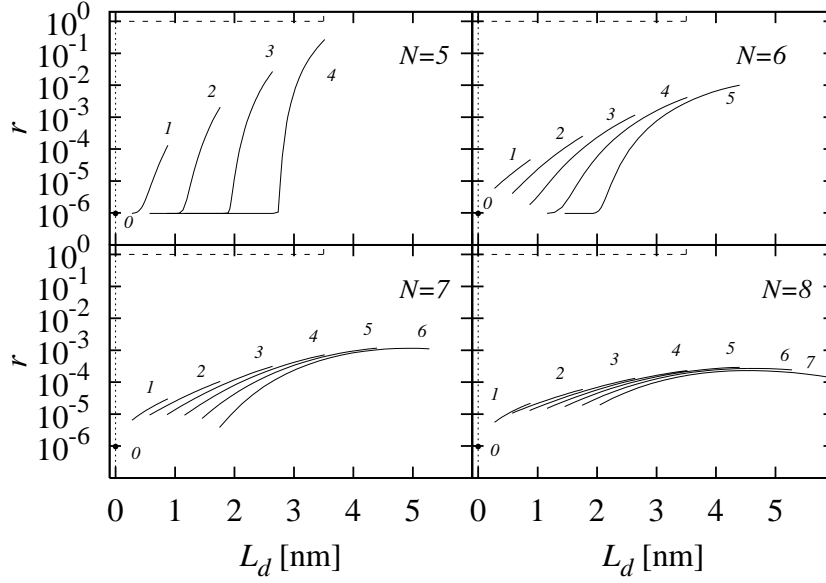


Figure 3: The ratio r of probabilities to bind forward and backward at the -7 pN stall force as a function of the horizontal projection L_d of the docked neck linker. The four boxes correspond to different values of N , and the different lines in the boxes correspond to different numbers N_d of docked segments. The preferred range of $r > 1$ and $L_d < 3.5$ nm can be seen in the top left corner of each box.

3 Results

We evaluated the integrals numerically for four integer values of N between 5 and 8. N_d took values between 0 and $N - 1$, so that we could compare the situation $N_d = 0$, where neck linker docking plays no role in the searching of the binding site, to various neck linker docking geometries. Although for completeness we varied the horizontal projection L_d of the docked neck linker from $0.4N_d l_K$ to $N_d l_K$, only values below 3.5 nm are acceptable since the kinesin head has a diameter of around 4 nm [1].

The results for the characteristic forward binding time t_f at the -7 pN stall force are presented in Fig. 2. All the curves decrease monotonically on the interval $L_d \in [0, 3.5\text{nm}]$. Thus, if we want to find the fastest forward step it is enough to look at the curves at $L_d = 3.5$ nm. The rectangular areas in the bottom left corners of the four boxes indicate the desired range of $t_f < 0.3$ s and the allowed regime of $L_d < 3.5$ nm.

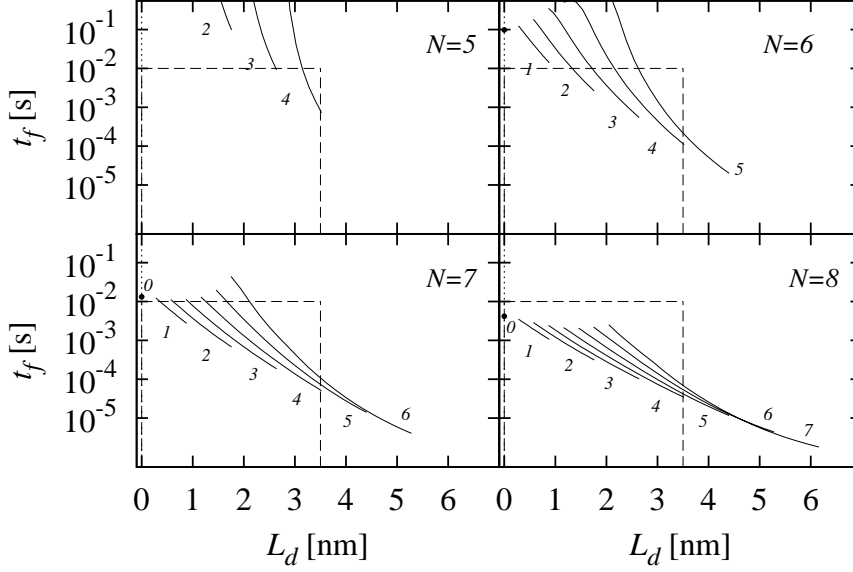


Figure 4: The same as Fig. 2, but at zero load, and the experimentally acceptable range is $t_f < 0.01$ s.

We used $k_b = 20 \text{ s}^{-1} \mu\text{M}^{-1}$ for the rate constant of MT binding [25, 9]. None of the curves passes through the desired area. We can make them do so by increasing k_b (which would simply shift them downwards). This can be justified by noticing that the $k_b \approx 20 \text{ s}^{-1} \mu\text{M}^{-1}$ value was measured for free kinesins in solution. However, in our case the tethered head is diffusing in the close vicinity of the MT, where electric fields are not fully screened and local attractive interactions might be significant, which can lead to an effectively elevated value of k_b . A threefold increase seems sufficient to make some curves just pass through the desired area for $N \geq 6$. A less feasible tenfold increase would, however, be necessary for $N = 5$.

In the r vs. L_d plots (Fig. 3) the value of k_b does not play any role (see Eq. (10)). All the curves for $N \geq 6$ are orders of magnitudes below $r = 1$, the value, which would be the expected at the stall force, if each forward binding resulted in a forward step, and each backward binding in a backward step. Obviously, there must exist some rectification mechanism that makes the completion of a backward steps less likely (*e.g.*, by reducing the ADP dissociation rate from the rear head) and increases the value of r to 1, but this is not the subject of our investigation.

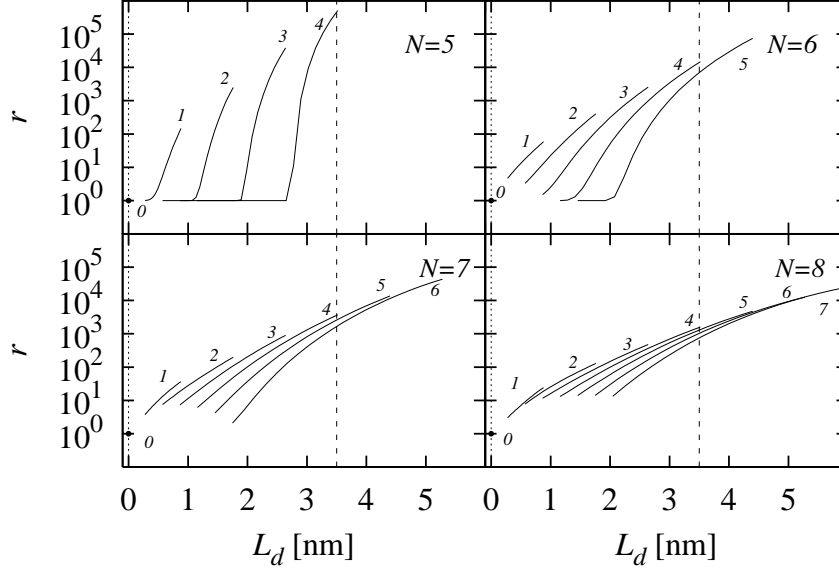


Figure 5: The same as Fig. 3, but at zero load.

For comparison we repeated the calculations at zero load as well (Figs. 4 and 5). These results indicate that for many N , N_d , and L_d combinations t_f is below the 0.01 s limit imposed by the experiments, even at $k_b = 20 \text{ s}^{-1} \mu\text{M}^{-1}$. Also, the values of r for $L_d = 3.5 \text{ nm}$ are orders of magnitude larger than 1, so with neck linker docking backward steps are highly improbable even without any rectification, in accordance with the experiments. Nevertheless, as r can never be smaller than 1 at zero load, the same rectification mechanism that helps at the stall force is also able to make the completion of backward steps rather unlikely in the unloaded situation.

4 Conclusions

As the results indicate kinesin under no load could march along MT in the forward direction even without neck linker docking. Under the stall force, however, neck linker docking seems to be crucial to forward stepping, as for $N_d = 0$ (corresponding to no docking) the characteristic forward binding time t_f is way over the desired value of 0.3 s. If the binding rate constant k_b near the MT is not expected to be larger than its bulk value of $20 \text{ s}^{-1} \mu\text{M}^{-1}$ by more than a factor of

3, then we get very strict constraints for the neck linker: it should contain at least $N = 6$ Kuhn segments, and dock all along the head with a horizontal projection of $L_d = 3.5$ nm. Moreover, since the value of r quickly decreases as N is increased, the best strategy for kinesin to walk forward upto a loading force of -7 pN is to have a neck linker of about $N = 6$ Kuhn segments (corresponding to 13-14 amino acids), with $N_d = 4$ or 5 segments capable of docking along the head. These values are very close to those known from the structure of kinesin, suggesting that kinesin is a very finely tuned motor protein whose parameters are set to live up to the highest load possible. This coincidence not only validates our calculations, but also justifies the relevance of neck linker docking in the motility of kinesin.

5 Appendix

Here we derive the formula for $\rho_N^0(\vec{R})$, the three dimensional probability density of the end-to-end distance of a FJC with N segments at zero loading force. Since N can be quite small we are not allowed to use the long FJC approximation of a polymer chain.

Let $\rho(\vec{R})$ be any three dimensional probability density with spherical symmetry so that $\vec{R} = 0$ is the origin. Then the relationship between $\rho(\vec{R})$ and its projection $\tilde{\rho}(x)$ to the x axis is:

$$\rho(\vec{R}) = -\frac{1}{2\pi|\vec{R}|} \left. \frac{d\tilde{\rho}(x)}{dx} \right|_{x=|\vec{R}|} \quad (11)$$

Since the end of a rigid rod can only move on the surface of a sphere the three dimensional density for an $N = 1$ FJC is a Dirac delta function on the surface of a sphere with radius l_K : $\rho_1^0(\vec{R}) = \delta(l_K - |\vec{R}|)/(4l_K^2\pi)$. By substituting $\rho_1^0(\vec{R})$ into Eq. (11) and integrating it we get for $\tilde{\rho}_1^0(x)$ a constant function with a value of $1/(2l_K)$ and a support between $-l_K$ and l_K . After autoconvoluting this function N times to get $\tilde{\rho}_N^0(x)$, and then converting it back to $\rho_N^0(\vec{R})$ with the help of Eq. (11), we arrive at the desired formula.

6 Acknowledgments

This work was supported by the Hungarian Science Foundation (K60665) and the Human Frontier Science Program (RGY62/2006).

References

- [1] Block, S.M., 1998. Kinesin: What Gives? Cell 93, 5–8.

- [2] Carter, N.J., Cross, R.A., 2005. Mechanics of the kinesin step. *Nature* 435, 308–312.
- [3] Case, R.B., Rice, S., Hart, C.L., Ly, B., Vale, R.D., 2000. Role of the kinesin neck linker and catalytic core in microtubule-based motility. *Curr. Biol.* 10, 157–160.
- [4] Hackney, D.D., 1994. Evidence for alternating head catalysis by kinesin during microtubule-stimulated ATP hydrolysis. *Proc. Natl. Acad. Sci. USA* 91, 6865–6869.
- [5] Howard, J., 2002. *Mechanics of Motor Proteins and the Cytoskeleton*. Springer, Berlin/Heidelberg.
- [6] Howard, J., Hudspeth, A.J., Vale, R.D., 1989. Movement of microtubules by single kinesin molecules. *Nature* 342, 154–158.
- [7] Hua, W., Young, E.C., Fleming, M.L., Gelles, J., 1997. Coupling of kinesin steps to ATP hydrolysis. *Nature* 388, 390–393.
- [8] Hyeon, C., Onuchic, J.N., 2007. Mechanical control of the directional stepping dynamics of the kinesin motor. *Proc. Natl. Acad. Sci. USA* 104, 17382–17387.
- [9] Gilbert, S.P., Webb, M.R., Brune, M., Johnson, K.A., 1995. Pre-Steady-State Kinetics of the Microtubule-Kinesin ATPase. *Biophys. J.* 68, 357.
- [10] Guydosh, N.R., Block, S.M., 2006. Backsteps induced by nucleotide analogs suggest the front head of kinesin is gated by strain. *Proc. Natl. Acad. Sci. USA* 103, 8054–8059.
- [11] Hwang, W., Lang, M.J., Karplus, M., 2008. Force generation in kinesin hinges on cover-neck bundle formation. *Structure* 16, 62–71.
- [12] Kikkawa, M., Sablin, E.P., Okada, Y., Yajima, H., Fletterick, R.J., Hirokawa, N., 2001. Switch-based mechanism of kinesin motors. *Nature* 411, 439–445.
- [13] Ma, Y.Z., Taylor, E.W., 1995. Kinetic Mechanism of Kinesin Motor Domain. *Biochemistry* 34, 13242–13251.
- [14] Ma, Y.Z., Taylor, E.W., 1997. Interacting Head Mechanism of Microtubule-Kinesin ATPase. *J. Biol. Chem.* 272, 724–730.
- [15] Mather, W.H., Fox, R.F., 2006. Kinesin’s Biased Stepping Mechanism: Amplification of Neck Linker Zippering. *Biophys. J.* 91, 2416–2426.

- [16] Mori, T., Vale, R.D., Tomishige, M., 2007. How kinesin waits between steps. *Nature* 450, 750–754.
- [17] Rice, S. *et al.*, 1999. A structural change in the kinesin motor protein that drives motility. *Nature* 402, 778–784.
- [18] Rice, S., Cui, Y., Sindelar, C., Naber, N., Matuska, M., Vale, R., Cooke, R., 2003. Thermodynamic Properties of the Kinesin Neck-Region Docking to the Catalytic Core. *Biophys. J.* 84, 1844–1854.
- [19] Schief, W.R., Howard, J., 2001. Conformational changes during kinesin motility. *Curr. Opin. Cell Biol.* 13, 19–28.
- [20] Schuler, B., Lipman, E.A., Steinbach, P.J., Kumke, M., Eaton, W.A., 2005. Polyproline and the “spectroscopic ruler” revisited with single-molecule fluorescence. *Proc. Natl. Acad. Sci. USA* 102, 2754–2759.
- [21] Sindelar, C.V., Budny, M.J., Rice, S., Naber, N., Fletterick, R., Cooke, R., 2002. Two conformations in the human kinesin power stroke defined by X-ray crystallography and EPR spectroscopy. *Nat. Struct. Biol.* 9, 844–848.
- [22] Skiniotis, G., Surrey, T., Altmann, S., Gross, H., Young-Hwa Song, Mandelkow, E., Hoenger, A., 2003. Nucleotide-induced conformations in the neck region of dimeric kinesin. *EMBO J.* 22, 1518–1528.
- [23] Vale R.D., 2003. The molecular motor toolbox for intracellular transport. *Cell* 112, 467–480.
- [24] Vale, R.D., Fletterick, R.J., 1997. The Design Plan of Kinesin Motors. *Annu. Rev. Cell Dev. Biol.* 13, 745–77.
- [25] Valentine, M.T., Gilbert, S.P., 2007. To step or not to step? How biochemistry and mechanics influence processivity in Kinesin and Eg5. *Curr. Opin. Cell Biol.* 19, 75–81.
- [26] Yildiz A., Tomishige M., Vale, R.D., Selvin, P.R., 2004. Kinesin Walks Hand-Over-Hand. *Science* 303, 676–678.